Analysis and mitigation of systematic errors in spectral shearing interferometry of pulses approaching the single-cycle limit [Invited]

Jonathan R. Birge* and Franz X. Kärtner

Department of Electrical Engineering and Computer Science Research Laboratory of Electronics, Massachusetts Institute of Technology, 77 Massachusetts Avenue, Cambridge, Massachusetts 02139, USA
*Corresponding author: birge@mit.edu

We derive an analytical approximation for the measured pulse width error in spectral shearing methods, such as spectral phase interferometry for direct electric-field reconstruction (SPIDER), caused by an anomalous delay between the two sheared pulse components. This analysis suggests that, as pulses approach the single-cycle limit, the resulting requirements on the calibration and stability of this delay become significant, requiring precision orders of magnitude higher than the scale of a wavelength. This is demonstrated by numerical simulations of SPIDER pulse reconstruction using actual data from a sub-two-cycle laser. We briefly propose methods to minimize the effects of this sensitivity in SPIDER and review variants of spectral shearing that attempt to avoid this difficulty. © 2008 Optical Society of America

OCIS codes: 320.7100, 120.5050.

1. INTRODUCTION
Steady progress in ultrafast laser sources over the past several decades has led to the recent development of robust sources of few-cycle laser pulses. Sub-two-cycle pulses can now be directly produced from oscillators, and sources of single-cycle pulses are under development [1,2]. Furthermore, as few-cycle lasers are increasingly used to drive attosecond extreme-UV and x-ray pulses, these applications will require an extremely accurate and precise characterization of the few- and single-cycle pulse envelopes used to drive the high harmonic generation process [3].

The technology for measuring ultrashort optical pulses must, of course, keep pace with the lasers themselves, and few- and single-cycle pulses present unique difficulties in this regard. The most obvious difficultly in a few-cycle pulse measurement stems from the tremendous bandwidths involved. All self-referenced pulse characterization methods involve nonlinear operations of some sort [4], and in the case of few-cycle pulses one essentially has to implement a specialized analog optical switch capable of operating with hundreds of terahertz of bandwidth. Any bandwidth filtering is especially relevant for techniques where the amplitude of the trace is a critical parameter, such as interferometric autocorrelation (IAC) [5] and frequency resolved optical gating (FROG) [6].

As pulses become shorter, the time scales of nonidealities do not always scale with them. For example, the relative delays of satellite pulses due to secondary reflections off dispersion-compensating mirrors do not scale with the main pulse width. In fact, if anything they inversely scale to the pulse width as mirrors become thicker to accommodate a wider spectral range. The spectral phase oscillation periods caused by such delays are usually on the or-

der of 5–10 THz. Thus, as bandwidths approach 200 THz and beyond, the time-bandwidth product required for a full characterization on even a well-compressed pulse can exceed 20.

In addition, the extreme bandwidths involved result in a higher-order material dispersion playing a significant role in pulse shaping, yielding pulses that are typically highly asymmetrical. As such, the commonly used technique of IAC, which is relatively insensitive to pulse asymmetries [7], can miss details. The squared intensity operation inherent to IAC greatly suppresses the effect of satellite pulses, for instance. As such, iterative reconstructions based on IAC (e.g., [5]) may fail to properly converge in the presence of noise when higher-order dispersive effects are significant.

One of the dominant characterization methods for very short pulses is spectral phase interferometry for direct electric-field reconstruction (SPIDER). In many ways, spectral shearing interferometry is uniquely suited to the task of measuring few- and single-cycle pulses. However, there is a calibration sensitivity with standard SPIDER (and many of its variants) that needs to be taken into consideration for pulses on the order of a single cycle.

We begin by briefly explaining the principle behind spectral shearing and its advantages in the few-cycle regime. Due to its importance to both accuracy and sensitivity, we discuss the importance of choosing a proper shear frequency and the considerations for doing so. Next, we analyze the sensitivity of the measurement to the delay reference inherent to spectral shearing, deriving an analytical result and simple scaling law. We show that relative measurement errors quadratically scale with the pulse bandwidth, leading to extreme sensitivity to calibration errors as pulse widths decrease past a few optical

cycles. We then illustrate this principle on experimental data from a sub-two-cycle oscillator, showing that a standard SPIDER apparatus would require mechanical stability far exceeding the scale of the wavelengths involved. Finally, we conclude by suggesting ways to mitigate the sensitivity and survey some recent alternative spectral shearing methods that attempt to eliminate it.

Our focus on spectral shearing is not meant to imply that we feel it is alone in presenting challenges to the characterization of pulses approaching a single cycle. In fact, our feeling is that spectral shearing is otherwise so well-suited to handling such pulses that it is worth examining these issues in some detail.

2. SPECTRAL SHEARING INTERFEROMETRY

A. Theory

SPIDER was developed by Iaconis and Walmsley in 1999 [8]. It is a modification of spectral interferometry, where both interfering components are obtained from the input pulse and are slightly shifted in frequency. This obviates the need for the reference pulse that is required in standard spectral interferometry. Called spectral shearing interferometry, this general idea represents a fundamentally unique mode of pulse measurement in that it directly observes interference between two adjacent frequency components. As such, it can be an extremely robust and direct method that avoids the need for iterative inversion algorithms.

Figure 1 shows a conceptual schematic of SPIDER. While the practical details greatly vary, all spectral shearing methods involve a nonlinear interferometer, whereby one arm experiences a different frequency shift than the other. Interference is observed between the two by putting some sort of phase shift on one of the arms. In the case of standard SPIDER, a linear phase shift is realized by interferometrically delaying the two pulse copies by τ.

By upconverting the pulse to be measured with a pair of frequencies separated by Ω, any original wavelengths in the pulse that are separated by this "shear" frequency are mapped to the same wavelength in the output. One may thus directly observe the phase delay between two nearby wavelengths and thereby the spectral dispersion. In standard SPIDER, the spectrally resolved output is given by [8]
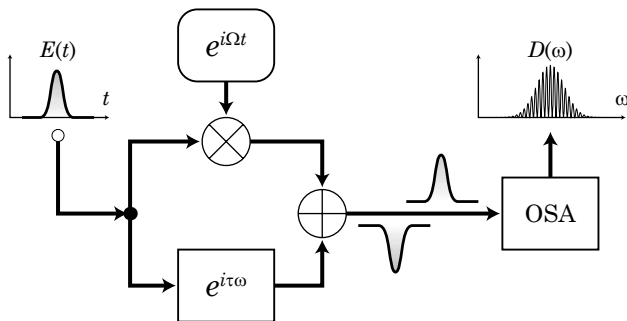

Fig. 1.   Conceptual schematic of SPIDER. This model intentionally abstracts away several practical details, such as the fact that, in practice, both pulse copies are upconverted by slightly different optical frequencies. However, these details are not important to an analysis of SPIDER.

$$D(\omega) = |E(\omega - \Omega)|^2 + |E(\omega)|^2 + 2|E(\omega - \Omega)E(\omega)|$$
$$\times \cos[\underbrace{\phi(\omega - \Omega) - \phi(\omega)}_{\phi'(\omega - \Omega/2)\Omega + O[\Omega^2]} + \tau\omega],$$

(1)

where $E(\omega) = |E(\omega)|e^{-i\phi(\omega)}$ is the upconverted spectrum of the pulse and τ is the delay between the two upconverted copies. [In practice $E(\omega)$ will be shifted in frequency from the fundamental, but its phase will be identical and its phase is all we are concerned with.] The oscillating cosine "carrier" fringe is the only element of interest, and its phase encodes a finite difference of the pulse spectral phase approximately proportional to the spectral group delay. The method for isolating this phase is beyond the scope of this paper and is not important to our end here. It suffices to mention that as long as τ is sufficiently large, the fringe phase may be reliably extracted by standard signal processing techniques. Since the initial development of SPIDER, many variants of spectral shearing interferometry have been invented but all share the same fundamental property of generating a carrier fringe in some domain (perhaps in space or time, if not frequency), which is shifted in proportion to the finite difference of the spectral phase $\phi(\omega - \Omega) - \phi(\omega)$. As such, spectral shearing interferometry essentially "samples" the spectral phase (up to a constant phase) with a discretization of Ω.

B. Application to Few-Cycle Pulses

The spectral shearing approach has three salient features relevant in the context of few-cycle pulses. First, the upconversion of the short pulse with a monochromatic field is fundamentally easier to perform than the full second-harmonic operation inherent to IAC and FROG. To begin with, the output relative bandwidth is roughly half that of the input as the spectrum is simply shifted and is not convolved with itself as in the case with second-harmonic-based methods. Most importantly, however, only one of the field components in the nonlinear operation contains the full bandwidth, which greatly facilitates phase matching; type II upconversion can be engineered to have a significant bandwidth in one of the input fields with a narrow bandwidth in the other, a perfect match for spectral shearing interferometry (see [9] for an illustration of this).

A second advantage comes from the use of phase to encode the spectral group delay. The spectral signal in Eq. (1) produced by SPIDER can be viewed as a carrier wave that is frequency modulated by a signal proportional to the spectral group delay. Much as frequency modulation is more robust to interference than amplitude modulation for a given signal power [10], this modulation scheme renders SPIDER methods relatively impervious to phase-matching bandwidth effects, as well as being highly immune to experimental noise. This noise tolerance was observed by Gallman *et al.* in [11] and by Jensen and Anderson in [12]. Robustness to noise is especially important given the relatively low efficiency of most spectral shearing embodiments, wherein much of the measured light is thrown away to create the chirped upconverting signal. The phase modulation scheme also makes spectral shearing tolerant to the presence of unwanted signals

(such as the fundamental pulse or higher diffraction orders from a grating spectrometer) that become increasingly difficult to suppress as bandwidths exceed an octave.

Last, spectral shearing directly measures spectral phase rather than the effects of it on the pulse envelope. Together with the aforementioned noise immunity of the encoding scheme, this makes spectral shearing methods extremely sensitive to the kind of pulse asymmetries and secondary pulses that are common in few-cycle lasers.

However, one issue that the original SPIDER does share with its correlation-based cousins (e.g., IAC) is that it requires the measured pulse to be split and delayed. For pulses approaching an octave of bandwidth, it is not yet possible to implement a dispersionless beam splitter, and the dispersion of the beam splitter is imprinted on the SPIDER measurement. Fortunately, this is not fundamental to spectral shearing; a few methods, to be discussed later, have been developed that involve nothing but reflections for the measured pulse.

C. Choice of Shear Frequency
The shear frequency Ω plays a critical role in both determining the sensitivity as well as the accuracy of a SPIDER measurement. Since it is the frequency spacing at which we concatenate the spectral phase, it determines the number of points at which we sample our spectrum over its bandwidth. According to the Shannon sampling theorem, the temporal window that we can handle without aliasing is the reciprocal of twice the shear. The time-bandwidth product that can be resolved is therefore $\Delta\omega/2\Omega$.

Since the modulation of the SPIDER fringe in Eq. (1) is proportional to the shear, one maximizes the signal-to-noise ratio of a spectral shearing measurement by choosing the largest shear that will avoid aliasing. As will be shown later, this also results in the least sensitivity to calibration errors. However, how can one determine, *a priori*, what that is? In theory, there is no way to know without actually making a measurement. Normally when one samples a signal, the bandwidth is known. However, in this case the "bandwidth" is the temporal extent of the pulse, and there is no reliable way to know that without having already done a pulse characterization. In practice, however, one generally knows the range of dispersion expected. Furthermore, one can fairly assume that structures in the power spectral density will coincide with oscillations in the spectral phase. In most cases, especially with few-cycle pulses, it is the latter that determines the required spectral sampling resolution. Thus, picking a shear that is sufficient to resolve the features of the amplitude spectrum will usually suffice. If in doubt, a sequence of shears can be used to effectively verify sufficient sampling.

Most lasers produce pulses with satellite structures and pedestals, to some extent or another. As such, in a properly performed measurement of a well-compressed pulse, with the spectral features sufficiently sampled, the vast majority of the energy is contained in a relatively small region of the resolvable temporal window. Given such a result, it is tempting for the user to assume that a larger shear can be safely used, with the argument being

that if the power outside the main pulse region is negligible, it will not hurt to ignore its effects when aliased. However, what may appear negligible in intensity when well-separated may have a significant effect when coherently added to the main pulse. Consider the case of a measurement where a pulse has distant satellite pulses that are no more than 1% of the intensity of the main pulse. Increasing the shear enough to alias the pedestal onto the main pulse can potentially result in 20% relative changes in the main pulse on an intensity basis. In general, the only way to verify sufficient sampling is to take another measurement at a different resolution.

3. SPECTRAL SHEARING DELAY SENSITIVITY

A. Pulse Width Error Scaling
Unfortunately, the advantages enumerated herein come at a certain cost. To gauge the phase of the fringe in Eq. (1) we must know the nominal period of the fringe, given by $1/\tau$. Of course, all ultrafast measurement techniques contain inherent length references that must be calibrated (such as the distance traveled by a delay stage in an autocorrelation or the spectrometer grating period in any spectrally resolved method). In most methods, the calibrations affect the measurement in a proportional way. However, it turns out that an error $\delta\tau$ in the interpulse delay τ will result in an additive measurement error, and thus this calibration becomes increasingly sensitive as the pulses become shorter.

In this section we derive a rough scaling law for the worst case error δt in the measured pulse width as a function of $\delta\tau$ by considering the characterization of a Gaussian pulse with a spectral $1/e^2$ half-width of $\Delta\omega$ [a figure that we use for mathematical simplicity and which is within 10% of the commonly used full-width at half-maximum (FWHM)]. We assume that the pulse we are measuring is solely dispersed by an amount of second-order dispersion given by ϕ'', and we are concerned with the error in estimating the pulse width in the presence of a given uncertainty $\delta\tau$ in the interpulse delay. The complex spectrum of the pulse is given by

$$E(\omega) = e^{-(\omega/\Delta\omega)^2 + (1/2)i\phi''\omega^2}. \tag{2}$$

From Eq. (1) we can see that any unaccounted delay $\delta\tau$ occurring between the two upconverted pulses will be associated, to first order, with the group delay and thus interpreted by the reconstruction as an erroneous linear group delay:

$$\delta\phi'(\omega) = \frac{\delta\tau\omega}{\Omega}. \tag{3}$$

Taking the derivative of both sides of Eq. (3) with respect to ω gives us an expression for the erroneous dispersion contributing to the measurement as a result of the delay error:

$$\delta\phi'' = \frac{\delta\tau}{\Omega}. \tag{4}$$

To consider the effect of this extra dispersion we begin with the well-known result (see [13], for example) for the temporal width (where we have translated the formula so that it is in terms of $1/e^2$ width) of a pulse broadened by the second-order dispersion,

$$T = T_0 \sqrt{1 + \left(\frac{\phi'' \Delta\omega}{2} \right)^2}, \qquad (5)$$

with T and T_0 the dispersed and Fourier limited widths, respectively. The actual measured pulse width, $T + \delta T$, can be written by replacing the dispersion in Eq. (5) with the measured dispersion $\delta\phi'' + \phi''$. Using the expression for $\delta\phi''$ given in Eq. (4), this means that the pulse width actually measured is simply

$$T + \delta T = T_0 \sqrt{1 + \left(\frac{\delta\tau \Delta\omega}{2\Omega} + \frac{\phi'' \Delta\omega}{2} \right)^2}. \qquad (6)$$

We consider the scenario where we erroneously measure a chirped pulse to be shorter than its true width. This implies that we consider the situation where ϕ'' (the true dispersion) is enough to significantly broaden the pulse, and $\delta\tau/\Omega$ (the erroneous dispersion added by the measurement) is of the opposite sign so as to diminish our estimate. Because of the second-order nature of broadening in Eq. (6), the measured pulse width can be very close to transform limited and yet still include enough dispersion such that the effects of extra delay are well approximated by a linear treatment of the dispersion curve. To derive a rough scaling law of the sensitivity of the measurement, then, we consider the first-order change in Eq. (6) to $\delta\tau$. Performing a series expansion of Eq. (6) with respect to $\delta\tau$ and then solving for δT gives

$$\delta T = \left(\frac{\phi''}{\sqrt{4/\Delta\omega^4 + (\phi'')^2}} \right) \left(\frac{\delta\tau \Delta\omega}{\Omega} \right) + O[\delta\tau^2]. \qquad (7)$$

Strictly speaking, this first-order expression is only accurate for $\phi'' \gg -\delta\tau/\Omega$, but it turns out to be off by no more than 25% as long as $|\phi''| > |\delta\tau/\Omega|$. However, this expression is only an accurate prediction if we can estimate the actual dispersion of the pulse (as in the case of an intentionally chirped pulse), and we know that our delay error is small relative to it. Nonetheless, the prefactor is close to one for any significant actual chirp (the case we must worry about). For example, it is already about 0.45 for a pulse that is 12% wider than its transform limit. Therefore, we have a worst-case error that roughly scales as

$$\delta T \approx \frac{\Delta\omega}{\Omega} \delta\tau. \qquad (8)$$

The final result is rather intuitive and simply states that the absolute measurement error is approximately the uncertainty in the interpulse delay times the dimensionless quantity $\Delta\omega/\Omega$, found earlier to be proportional to the number of spectral samples, and thus also the time-bandwidth product. Again, this formula is an overestimate in the case where our measured pulse is transform limited (since $\phi'' = -\delta\tau/\Omega$). However, in reality this is somewhat offset by the fact that very short pulses usually have residual higher-order dispersion that cannot be per-

fectly compensated. In practice, this formula is thus fairly accurate as illustrated in Section 5.

A corollary of Eq. (8) is that the relative error in measurement scales with the square of the spectrum:

$$\frac{\delta T}{T + \delta T} \approx \frac{\Delta\omega^2}{2\Omega} \delta\tau, \qquad (9)$$

which was obtained by multiplying both sides of Eq. (8) by the bandwidth and using the Fourier uncertainty relation, where we have assumed that the pulse as measured is close to the Fourier limit.

One might hope that as pulses become shorter, the number of sampling points could be kept constant by increasing Ω in proportion to the bandwidth. Unfortunately, this is generally not the case for few-cycle pulses as explained in Section 4. As bandwidths increase in an optical system, the temporal window that we must resolve becomes limited by the pulse pedestal and secondary pulses, and at this point the shear must remain fixed and the number of sampling points must grow with the spectrum. Thus, while Eq. (9) would indicate a linear scaling with the bandwidth if everything in a laser scaled in unison, in practice this is not the case, and we must conservatively assume that the scaling is square in the bandwidth.

B. Tolerance on Delay Uncertainty for Compressed Pulses

In Subsection 3.A, a rough intuitive scaling law was derived, where several approximations were made, most notably that some residual measured dispersion remains. We now address the situation where the pulse has been perfectly compressed according to the measurement. In this case, we can exactly determine how much delay uncertainty can be allowed while still being assured of having a compressed pulse to within some tolerance. Taking 5% as our tolerance for deviation from the transform limited width, the allowable delay uncertainty $\delta\tau_{5\%}$ can be found without approximation by taking $T \to 1.05 T_0$ and $\phi'' \to \tau_{5\%}/\Omega$ in Eq. (5). Solving for $\delta\tau_{5\%}$ gives

$$\delta\tau_{5\%} = 0.64 \frac{\Omega}{\Delta\omega^2} = 0.32 \frac{T_0}{N}, \qquad (10)$$

where N is the number of spectral sampling points within the bandwidth (twice the time-bandwidth product).

4. CALIBRATION OF SPIDER IN PRACTICE

A. Required Precision

By way of example, we consider the prospect of measuring a single-cycle Gaussian pulse whose full-width $1/e^2$ bandwidth is $\Delta f = 282$ THz. Using a shear of $\Omega = 2\pi \times 5$ THz will result in a resolvable time-bandwidth product of roughly 30 (using the FWHM values). Based on our experience with few-cycle lasers, this would be a conservative resolution requirement for a single-cycle laser. In practice, for few-cycle pulses and below, the spectra tend to be highly structured, with the number of spectral samples required on the order of 20–100. See, for example, [2,14,15]. For a standard SPIDER configuration, this shear implies a de-

lay of around $\tau = 200$ fs. (This is to ensure that sufficient chirp is used such that the upconversion can be considered a pure shift.)

According to Eq. (10), in order to limit our maximum error to within 5% (roughly 0.14 fs), the interpulse delay error must be measured and maintained to within 25 attoseconds (as), corresponding to a delay of 7.5 nm. Recently, the shortest isolated pulses ever published [2] were measured using a modified SPIDER (modified to amplify the chirped pulses) with a shear of $\Omega = 2\pi \times 4.11$ THz, which implies a tolerance of about 21 as or 6.3 nm.

B. Sources of Delay Error
There are several avenues through which unaccounted for interpulse delays can arise in practice with a standard SPIDER setup. It is our hope that by enumerating them, researchers can mitigate their effects simply by keeping aware of them during the construction and operation of a SPIDER apparatus.

1. Delay calibration. The most obvious source of delay error is simple error in the calibration measurement. In our example, a relative precision measurement of 0.025% is required over 4 orders of magnitude. This is not exactly trivial but certainly achievable using interferometric means. As pointed out by Dorrer in [16], however, errors in the calibration of the spectrometer will translate into errors in the effective τ used. Thus, the spectrometer used in the measurement must be free of relative errors (over the pulse bandwidth) to within the same precision unless the errors can be canceled out by self-calibration (see below).

2. Thermal drift. A perhaps more worrisome source of delay error is thermal drift in the setup over time. Taking, for instance, the thermal expansion coefficient of aluminum (2.5×10^{-5}) and considering a relatively small Michelson interferometer with arm lengths of 2.5 cm, a temperature differential of $0.006\,°C$ between the two arms will cause a problematic change in delay. Uniform temperature shifts should not pose a problem; an interferometer of any size will be able to withstand a uniform temperature shift of up to $5\,°C$ before a noticeable delay occurs.

3. Alignment drift. Another source of delay is alignment drift of the incoming laser beam. Any misalignment in the beam will change the delay by τ times the cosine of the angle error. Assuming perfect alignment to begin with, this means that 15 mrad of change in laser pointing will cause noticeable errors for a single-cycle pulse. This is not an issue for passive stability of the laser but suggests that any tuning of the laser itself will require a recalibration of the SPIDER for few-cycle pulses.

4. Unmeasured path difference. Calibrating the interpulse delay often involves changing the experimental configuration somewhat [such as rotating the nonlinear crystal to produce a type I second-harmonic generation (SHG)]. Thus, care must be taken such that the measured delay is identical to the delay actually used. For example, if the SHG interference fringe is to be used to calibrate out the delay phase, it is even more important that the total distance traveled by the beam not change from the calibration configuration to the measurement configura-

tion. This could be a potential issue with noncollinear arrangements, where the SHG geometry will be fundamentally different than that used for the sum-frequency generation (SFG) employed during the actual measurement. Assuming the two pulse copies are only known to be collinear to within 1 mrad, changing the total propagation length by more than 2 cm would put the unknown delay out of tolerance for a single-cycle pulse.

C. Avoiding Delay Error
The most obvious lesson from the preceeding is that for a few-cycle pulse characterization with standard SPIDER, a new calibration should be performed immediately preceding each measurement to avoid issues of delay stability, leaving only the matter of delay measurement.

Fortunately, the issue of the delay calibration becoming enmeshed with the spectrometer calibration has been previously addressed. In [16], Dorrer shows that if the delay is calibrated using the interference of the individual second harmonic of each pulse copy using the same spectrometer, which will be used for the SPIDER measurement, then any spectrometer error will cancel out. When making measurements of few-cycle pulses using a standard SPIDER, it is thus imperative that the delay phase be removed in such a self-calibrated way. Otherwise, the delay calibration sensitivity translates into the more difficult issue of calibrating the spectrometer to within at least 4 orders of magnitude relative precision and measuring a fringe period to the same degree. One potential difficulty with this is that the SHG signals must cover the same bandwidth as the sheared upconverted signals. Given the difference in phase matching between the SHG and SFG signals, this could present a difficulty and may explain why a self-calibrating SPIDER measurement has not been demonstrated (to our knowledge) for a few-cycle pulse.

Ideally, for the sake of avoiding any possibility of delay drift, the calibration of the delay would be simultaneously done with the measurement. Dorrer has developed a method [17] to do just that by taking advantage of multiple diffraction orders in a grating spectrometer. His method is also self-calibrating in the sense described herein, since both the calibration fringe at the fundamental frequency and the SPIDER fringe at the upconverted frequency share the same wavelength range on the detector. When standard SPIDER is used, and when the pulse lengths are not so short that dispersion is an issue, beam splitting may be done using an etalon (as in [18]) to eliminate issues of thermal sensitivity.

Last, the effects of beam pointing can be greatly mitigated by ensuring that the interferometer generating the pulse copies is well-aligned such that pointing errors introduce only second-order delay errors. Collinear SPIDER implementations, which rely on pulse shaping to create the pulse copies [19], and those that use no delay (see Subsection 6.C) have an advantage in this regard.

5. NUMERICAL SIMULATIONS
In the derivation of Subsection 3.A, we relied on a Gaussian analysis. However, the spectra in real lasers tend to have more complicated spectra that are often
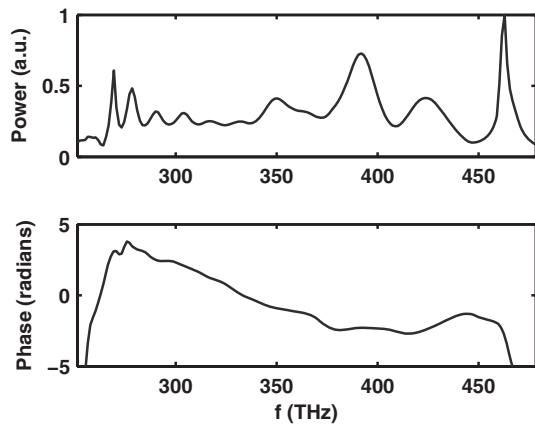
Fig. 2.   Spectral power density and spectral phase for an actual sub-two-cycle Ti:sapphire oscillator measured with 2DSI.

closer to rectangular than Gaussian. To test the validity of our analytical results, we simulated the effect of a spurious delay $\delta\tau$ on a standard SPIDER measurement of a sub-two-cycle pulse, using spectral data from an actual Ti:sapphire laser.

We recently constructed a sub-two-cycle ring laser [20] and characterized it using two-dimensional spectral shearing interferometry (2DSI) [21], the spectrum and phase of which are shown for reference in Fig. 2. The power and phase spectrum are both rather oscillatory, owing to self-phase modulation (SPM) and extra reflections from the intracavity dispersion compensating mirrors. To resolve the finest oscillations, a shear of 4.5 THz was required. Using the spectral phase measured by 2DSI, we simulated the case where a standard SPIDER measurement shows a very slightly chirped pulse of 4.94 fs FWHM. This is nearly as compressed as can be achieved by a bulk material compensation. We then computed what the actual pulse was, assuming a worst case interpulse delay error due to several lengths of extra path length. The envelopes were computed using a padded fast Fourier transform (FFT) of the complex spectrum, neglecting any carrier offset (since we are only interested in the pulse envelope). The pulse rms width (over a 40 fs window) and the FWHM were computed. The latter was calculated by
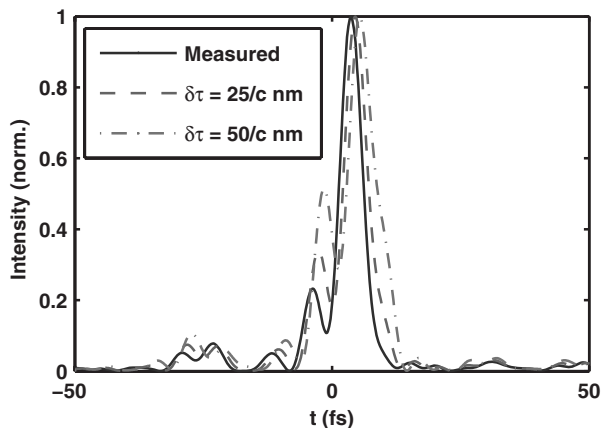
Table 1. Summary of Simulated Ti:sapphire Measurements

	Measurements (fs)	15 nm/c (fs)	$\delta\tau$ 30 nm/c (fs)	60 nm/c (fs)
FWHM	4.94	5.032	5.26	12.8
rms	10.95	11.31	11.85	13.31

using a Newton method to solve for the intersection of a cubic spline with the 50% point. The resulting pulses are shown in Fig. 3 with results tabulated in Table 1. (The rms widths are much larger due to significant satellite pulses and pedestal.)

Note that it only took an extra delay of 30 nm, or 100 as, to cause an error over 5%. Furthermore, this example was actually conservative in that the measured pulse was well-compressed and thus the nonlinear relation of the FWHM width to dispersion helped; the same data also imply that, had the actual pulse been 12.8 fs long, only 30 nm of spurious delay would have made it appear to be only 5.25 fs long. The point here is that if spectral shearing is used to measure pulses that are intentionally chirped (as in the case of pulses used in coherent control or those precompensated for material dispersion) the measurement will be maximally sensitive such that Eq. (8) is an accurate estimate.

To test the applicability of the analytical results from Subsection 3.A, the relative error was simulated for a range of $\delta\tau$ between 0 and 60 nm and compared with that predicted by Eq. (9), taking the $1/e^2$ half-width $\Delta\omega$ to be $2\pi\times 138$ THz (approximately half of the full range of the measured spectrum). The results are shown in Fig. 4. After enough dispersion, the FWHM behaves severely nonlinearly as subpulses grow past 50%. As anticipated by the fact that this pulse is nearly transform limited as measured, the linear scaling law overestimates the errors. However, the error is not large, and it is generally within a factor of 2 of the rms width. By comparison, the exact 5% tolerance predicted by Eq. (10) is $\delta\tau_{5\%}=81$ nm, a significant underestimate of that actually achieved. This is because Eq. (10) assumes a smooth spectrum with no

Fig. 3.   Simulated pulse intensity as measured (solid curve) and in truth (dashed and dashed–dotted curves) for the Ti:sapphire laser whose spectra are shown in Fig. 2, assuming delay errors of 25 and 50 nm.
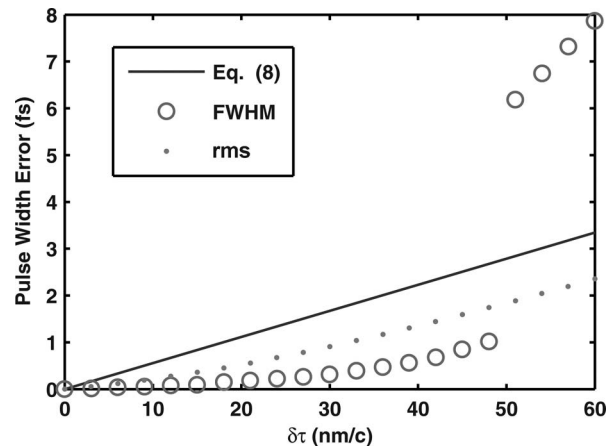

Fig. 4.   Measured pulse FWHM and rms widths of the pulse in Fig. 3 for a range of $\delta\tau$ values compared with that predicted by Eq. (8) using the half-width of the spectrum as $\Delta\omega$.

high-order dispersion. Thus, if our laser is representative, the sensitivity estimates given in Subsection 4.A may be conservative for a single-cycle laser.

6. ALTERNATIVE SPECTRAL SHEARING METHODS

We have already presented an outline of various ways to mitigate systematic errors related to spurious delays in spectral shearing. For cases where the sensitivity or pulse splitting of SPIDER cannot be tolerated, several alternative modes of spectral shearing have been developed in the past several years that address these issues.

A. Arbitrary Shear Methods

As previously discussed, the shear plays a crucial role in the sensitivity of the measurement. This applies to any spectral shearing method. Since the error δT is proportional to the absolute uncertainty $\delta \tau$, and not the relative uncertainty, the effect of calibration errors can be minimized by choosing as small a τ as possible while still allowing decoding of the fringe phase. Similarly, we want to choose as large an Ω as is consistent with the Nyquist criterion of the spectral phase.

In standard SPIDER, unfortunately, the delay and shear are linked through the dispersion used to produce the monochromatic signal used for upconversion. In [8] this relation is $\tau = -\Omega \phi''_{\text{chirp}}$. It can be shown that the amount of chirp needed to avoid artifacts is proportional to $1/\Omega^2$. However, the minimum requirement on τ is actually quite complicated, and it is best found empirically. Thus, SPIDER does not, in general, offer sufficient degrees of freedom to optimally choose τ and Ω.

However, there are several spectral shearing variants that do allow for independent selections of τ and Ω. The first to do so was homodyne optical technique (HOT) SPIDER [22], which uses a homodyne technique to allow two measurements against a local oscillator to be combined to yield a normal SPIDER trace. While this method requires a second source that covers the upconversion wavelengths, it also has the benefit of implicitly calibrating the delay. However, this method may be of limited use for very short pulses because of the requirement for a separate source with the same bandwidth but at twice the frequency (the main source can also be used, but this would be highly inefficient and against the point of homodyning).

B. Zero-Dispersion Methods

Another approach that is capable of arbitrary shears is zero-additional-phase (ZAP) SPIDER [23], developed by Baum *et al.*, which introduced the idea of using dual chirped pulses to upconvert a single short pulse. This means that the pulse to be measured never has to pass through any material (other than the thin nonlinear crystal before it is upconverted), and hence this method adds zero additional phase. To our knowledge, ZAP SPIDER was the first demonstration of a self-referencing pulse characterization method that involved no added dispersion to the measured pulse. One potential issue is that the noncollinear nature of ZAP SPIDER may present difficulties in measuring τ, at least in a self-calibrating way. Spa-

tially encoded arrangement (SEA) SPIDER [24] and 2DSI [21] also use two chirped pulses to avoid dispersion on the measured pulse, and furthermore both set the delay to zero. This brings us to another way to address the delay calibration, avoid it altogether.

C. Zero-Delay Methods

In the SPIDER interferogram, described in Eq. (1), the dense fringe created by the delay phase $\tau \omega$ allows for robust and unambiguous extraction of the $\phi(\omega) - \phi(\omega - \Omega)$ term in which we are interested. However, this carrier fringe need not be in the spectral domain; the phase shown in the lower arm of the SPIDER schematic in Fig. 1 does not have to be a function of optical frequency. In fact, having any component of it in the spectral domain is really the origin of the entire calibration sensitivity issue discussed in this paper.

To this end, SEA SPIDER, developed by Kosik *et al.* [24] and demonstrated for sub-10 fs pulses by Wyatt *et al.* [25], is a version of SPIDER that creates a fringe in the spatial domain on an imaging spectrometer. A related method, 2DSI developed by Birge *et al.* [21], uses a collinear output and creates a fringe in the time domain.

In theory, these two methods should be immune to the delay uncertainty errors discussed in this paper. However, in practice things may not be so simple. The error given in Eq. (8) is true for any spectral shearing method, even those with nominally zero delay between the two pulse copies. Thus, any incidental path length difference that occurs will contribute to measurement errors in exactly the same way as with standard SPIDER.

In the case of SEA SPIDER, the spatial fringe is created by sending the two upconverted pulses along separate routes in a plane before meeting at the spectrometer. This creates a spatially dependent delay in an axis perpendicular to the axis over which the spectrum is resolved. Any deviation of these pulses out of the plane, or delays incurred during their separate travels, will create a $\delta \tau$ that must be either calibrated or avoided to the same precision as for standard SPIDER. Furthermore, if the spectrometer grating axis is rotated with respect to the nominal spatial fringe, this will have the same effect as a delay and may have to be calibrated.

In 2DSI, the fringe is produced by scanning the phase of one of the chirped pulses, and a 2D fringe is produced as a function of wavelength and this phase. The only thing that matters in the 2DSI fringe is the absolute phase of the fringe at a given wavelength, and thus no calibration is needed. The cost of this is that 2DSI is incapable of single-shot measurements.

The two upconverted pulses in 2DSI originate from the same point and are collinear, so it should not be possible for a delay to occur between the pulse copies. However, misalignment and nonidealities in the imaging of the pulses into the spectrometer could potentially introduce an unwanted delay. Nonetheless, we have not seen any evidence of this after several measurements of few-cycle pulses [26,27]. In fact, we have recently directly measured a 4.9 fs pulse from an oscillator and verified it against both an IAC and a simulation of the laser [20,15,28].

D. Multiple Shearing

Finally, for those methods where multiple shears can be produced (and where changing the shear can be guaranteed to have no effect on the delay) the issue of delay calibration can be eliminated by making two or more measurements with different shear frequencies. By subtracting the phase of two spectral shearing measurements made with different shears, the phase of the delay drops out and one is essentially left with a SPIDER measurement performed with the difference in the shears. A novel version of SPIDER that relies on this principle for a continuum of shears was recently presented by Gorza *et al.* [29].

As long as one of the measurements is done with a shear that is consistent with the sampling theorem, the subsequent "calibration" measurements can be made with much larger shears, with the only requirement being that they are integer multiples of the shear used for the final measurement.

7. CONCLUSION

We have shown, through analysis and numerical simulation, that as pulses approach the single-cycle limit, the SPIDER technique involves a calibration that is exceedingly difficult. However, given the unique position of SPIDER as the only direct method of phase measurement, and given its inherent bandwidth advantages over other methods, it is worthwhile to search for mitigation strategies. We conclude that for most cases, awareness of the calibration sensitivity and careful adherence to the principle that calibrations must be done before every measurement are sufficient to yield accurate results. For extremely short pulses, however, it may be best to employ one of the variants of SPIDER discussed in Section 6 that remove the delay calibration issue.

ACKNOWLEDGMENTS

REFERENCES

1. T. R. Schibli, O. Kuzucu, J. Kim, E. P. Ippen, J. G. Fujimoto, F. X. Kärtner, V. Scheuer, and G. Angelow, "Towards single-cycle laser systems," IEEE J. Sel. Top. Quantum Electron. **9**, 990–1001 (2003).
2. E. Matsubara, K. Yamane, T. Sekikawa, and M. Yamashita, "Generation of 2.6 fs optical pulses using induced-phase modulation in a gas-filled hollow fiber," J. Opt. Soc. Am. B **24**, 985–989 (2007).
3. P. B. Corkum and F. Krausz, "Attosecond science," Nat. Phys. **3**, 381–387 (2007).
4. I. A. Walmsley and V. Wong, "Characterization of the electric field of ultrashort optical pulses," J. Opt. Soc. Am. B **13**, 2453–2563 (1996).
5. J. Nicholson, J. Jasapara, W. Rudolph, F. Omenetto, and A. Taylor, "Full-field characterization of femtosecond pulses by spectrum and cross-correlation measurements," Opt. Lett. **24**, 1774–1776 (1999).
6. D. Kane and R. Trebino, "Characterization of arbitrary femtosecond pulses using frequency-resolved optical gating," IEEE J. Quantum Electron. **29**, 571–579 (1993).
7. J. Chung and A. Weiner, "Ambiguity of ultrashort pulse shapes retrieved from the intensity autocorrelation and the power spectrum," J. Spec. Top. Quantum Electron. **7**, 656–666 (2001).
8. C. Iaconis and I. Walmsley, "Self-referencing spectral interferometry for measuring ultrashort pulses," IEEE J. Quantum Electron. **35**, 501–509 (1999).
9. I. A. Walmsley, "Characterization of ultrashort optical pulses in the few-cycle regime using spectral phase interferometry for direct electric-field reconstruction," in *Few-Cycle Laser Pulse Generation and its Applications*, F. Kärtner, ed. (Springer, 2004), pp. 265–291.
10. E. H. Armstrong, "A method of reducing disturbances in radio signaling by a system of frequency modulation," Proc. IRE **24**, 689–740 (1936).
11. L. Gallmann, D. Sutter, N. Matuschek, G. Steinmeyer, and U. Keller, "Techniques for the characterization of sub-10-fs optical pulses: a comparison," Appl. Phys. B **70**, S67–S75 (2000).
12. S. Jensen and M. Anderson, "Measuring ultrashort optical pulses in the presence of noise: an empirical study of the performance of spectral phase interferometry for direct electric field reconstruction," Appl. Opt. **43**, 883–893 (2004).
13. A. Yariv, *Optical Electronics in Modern Communications*, 5th ed. (Oxford U. Press, 1997).
14. K. Yamane, Z. Zhang, K. Oka, R. Morita, and M. Yamashita, "Optical pulse compression to 3.4 fs in the monocycle region by feedback phase compensation," Opt. Lett. **28**, 2258–2260 (2003).
15. H. M. Crespo, J. R. Birge, E. L. Falcão Filho, M. Y. Sander, A. Benedick, and F. X. Kärtner, "Non-intrusive phase-stabilization of sub-two-cycle pulses from a prismless octave-spanning Ti:sapphire laser," Opt. Lett., doc. ID 90799 (posted 14 March 2008, in press).
16. C. Dorrer, "Influence of the calibration of the detector on spectral interferometry," J. Opt. Soc. Am. B **16**, 1160–1168 (1999).
17. C. Dorrer, "Implementation of spectral phase interferometry for direct electric-field reconstruction with a simultaneously recorded reference interferogram," Opt. Lett. **24**, 1532–1534 (1999).
18. T. Shuman, I. A. Walmsley, L. Waxer, M. Anderson, C. Iaconis, and J. Bromage, "Real-time spider: ultrashort pulse characterization at 20 Hz," Opt. Express **5**, 134–143 (1999).
19. B. von Vacano, T. Buckup, and M. Motzkus, "Shaper-assisted collinear spider: fast and simple broadband pulse compression in nonlinear microscopy," J. Opt. Soc. Am. B **24**, 1091–1100 (2007).
20. J. R. Birge, H. M. Crespo, M. Sander, and F. X. Kärtner, "Non-instrusive sub-two-cycle carrier-envelope stabilized pulses using engineered chirped mirrors," in *Proceedings of the Conference of Lasers and Electro-Optics (CLEO)* (Optical Society of America, 2008).
21. J. R. Birge, R. Ell, and F. X. Kärtner, "Two-dimensional spectral shearing interferometry for few-cycle pulse characterization," Opt. Lett. **31**, 2063–2065 (2006).
22. C. Dorrer, P. Londero, and I. A. Walmsley, "Homodyne detection in spectral phase interferometry for direct electric-field reconstruction," Opt. Lett. **26**, 1510–1512 (2001).
23. P. Baum, S. Lockbrunner, and E. Riedle, "Zero-additional-phase SPIDER: full characterization of visible and sub-20-fs ultraviolet pulses," Opt. Lett. **29**, 210–212 (2004).
24. E. Kosik, A. Radunsky, I. Walmsley, and C. Dorrer, "Interferometric technique for measuring broadband ultrashort pulses at the sampling limit," Opt. Lett. **30**, 326–328 (2005).
25. A. S. Wyatt, I. A. Walmsley, G. Stibenz, and G. Steinmeyer,

"Sub-10 fs pulse characterization using spatially encoded arrangement for spectral phase interferometry for direct electric field reconstruction," Opt. Lett. **31**, 1914–1916 (2006).

26. J. R. Birge, R. Ell, and F. X. Kärtner, "Two-dimensional spectral shearing interferometry (2DSI) for ultrashort pulse characterization," in *Proceedings of the Conference of Lasers and Electro-Optics (CLEO)* (Optical Society of America, 2006).

27. J. R. Birge, R. Ell, and F. X. Kärtner, "Two-dimensional spectral shearing interferometry for few-cycle pulse characterization and optimization," in *Ultrafast Phenomena XV*, P. Corkum, D. Jonas, R. Miller, and A. Weiner, eds. (Springer, 2006), pp. 160–162.

28. M. Y. Sander, H. M. Crespo, J. R. Birge, and F. X. Kärtner, "Modeling of octave-spanning sub-two-cycle titanium:sapphire lasers: simulation and experiment," in *Proceedings of the Conference on Ultrafast Phenomena*, Stresa, Italy, June 2008.

29. S.-P. Gorza, P. Wasylczyk, and I. A. Walmsley, "Spectral shearing interferometry with spatially chirped replicas for measuring ultrashort pulses," Opt. Express **15**, 15168–15174 (2007).